Mapping and discrimination of networks in the complexity-entropy plane

Marc Wiedermann,[1,2,*] Jonathan F. Donges,[1,3] Jürgen Kurths,[1,2] and Reik V. Donner[1]
[1]*Potsdam Institute for Climate Impact Research, Telegraphenberg A31, 14473 Potsdam, Germany, EU*
[2]*Department of Physics, Humboldt University, Newtonstr. 15, 12489 Berlin, Germany, EU*
[3]*Stockholm Resilience Centre, Stockholm University, Kräftriket 2B, 114 19 Stockholm, Sweden, EU*
(Received 24 April 2017; published 17 October 2017)

Complex networks are usually characterized in terms of their topological, spatial, or information-theoretic properties and combinations of the associated metrics are used to discriminate networks into different classes or categories. However, even with the present variety of characteristics at hand it still remains a subject of current research to appropriately quantify a network's *complexity* and correspondingly discriminate between different types of complex networks, like infrastructure or social networks, on such a basis. Here we explore the possibility to classify complex networks by means of a statistical complexity measure that has formerly been successfully applied to distinguish different types of chaotic and stochastic time series. It is composed of a network's averaged per-node entropic measure characterizing the network's information content and the associated Jenson-Shannon divergence as a measure of disequilibrium. We study 29 real-world networks and show that networks of the same category tend to cluster in distinct areas of the resulting complexity-entropy plane. We demonstrate that within our framework, connectome networks exhibit among the highest complexity while, e.g., transportation and infrastructure networks display significantly lower values. Furthermore, we demonstrate the utility of our framework by applying it to families of random scale-free and Watts-Strogatz model networks. We then show in a second application that the proposed framework is useful to objectively construct threshold-based networks, such as functional climate networks or recurrence networks, by choosing the threshold such that the statistical network complexity is maximized.

DOI: 10.1103/PhysRevE.96.042304

I. INTRODUCTION

Many real-world systems are well represented by complex networks [1,2]. Examples include social systems, such as herds of one or more species of animals [3,4]; transportation systems, such as road networks [5,6]; or connectome networks, such as the human brain [7,8].

The structure of such networks is usually quantified by a set of topological [9], spatial [10], or information-theoretic [11] characteristics which measure certain properties of either distinct nodes (local characteristics) or the entire network itself (global characteristics). Specifically, the latter may be used to compare different kinds of networks as well as for categorizing a given set of networks into different classes [12]. The most prototypical example of such a discrimination would be the assignment of the small-world property to a given network (following Watts and Strogatz) depending on the numerical values of its clustering coefficient and average path length [13].

Other approaches have successfully distinguished between different classes of scale-free networks by means of characteristics associated with their degree distribution [14] or spatial networks by determining bias corrected versions of macroscopic network characteristics [15]. Further, networks have been assigned to so-called superfamilies based on the distribution of certain motifs that form their substructure [16]. One successful approach to quantify topological differences in networks of different types is based on examining their community structure and yields statistical properties within the communities that are unique to different types of networks under study [17].

However, while the large variety of present metrics allows for a quantification of a network's particular macroscopic and microscopic structure, it still remains a subject of current research to (i) assess the actual *complexity* of a network based on these sets of characteristics [18] and (ii) to determine distinct sets of properties for certain classes of networks, such as infrastructure or social networks, in order to objectively and comprehensively distinguish between them. While there exists a variety of such complexity measures [19], most of them are tailored to specific applications and have so far not been successfully applied to intercompare different types or classes of networks as in this respect they often lack a meaningful interpretation [20].

Contributing to the above issues, we introduce here a two-dimensional metric based on an entropic and an adjoint statistical complexity measure to distinguish different types of complex networks [21,22]. This approach was originally introduced to distinguish chaotic from stochastic systems in time series analysis and has been successfully applied to study, e.g., ordinal patterns in daily stream time series of river runoff [23]. Its purpose is to assign each system under study a position in a two-dimensional space spanned by an entropy and a statistical complexity measure, the latter being a product of entropy and Jenson-Shannon divergence with respect to a uniform distribution.

Here we transfer this concept from time series to the case of complex networks and redefine the above entropy and statistical complexity accordingly. Various definitions of network entropies or, more specifically, the underlying probability distributions have already been proposed. They may for example be computed in terms of the network's topological information content [24] or, quite commonly, its degree distribution [25–27]. Further definitions of entropy are

*marcwie@pik-potsdam.de

based on the assessment of network ensembles or randomized correspondents thereof [18,28]. However, particularly entropy measures that are based on the degree-distribution alone have been shown to have little discriminative power when applied to a heterogeneous set of graphs [29]. It is in contrast rather advisable to rely on local per-node definitions of network entropies [29,30].

One candidate for such a nodewise definition of entropy is based on the probability of a random walker to jump from a specific node to its neighbors in the network [31]. This notion of entropy is closely related to random walks which themselves are in their application and interpretation closely related with the assessment of a networks' navigability and, thus, complexity [10,32,33].

We apply our formalism to 29 real-world networks that are discriminated by context into the four types of social animal, social affiliation, transportation, and connectome networks. We show that for most cases the different types occupy distinct areas in the complexity-entropy plane. Thus, our formalism naturally distinguishes between different types of systems under study. We also apply the framework to two generic classes of benchmark networks, namely an ensemble of scale-free networks with varying power-law exponents and a set of networks constructed from the Watts-Strogatz model for different rewiring probabilities [13]. In a second application, we show that our complexity measure can be used to objectively construct threshold-based networks such as functional climate networks [34,35] or recurrence networks [36] by choosing a discrete network representation that maximizes statistical complexity.

The remainder of this paper is organized as follows: Section II presents the methodology that is put forward in this work and additionally introduces the kinds of networks that are studied in the two example applications. The corresponding results are presented in Sec. III and the work is ultimately concluded with an outlook in Sec. IV.

II. METHODS AND DATA

An unweighted network G with a set of N nodes labeled with integers $i = 1, \ldots, N$ and corresponding links between nodes can be represented by its $N \times N$ adjacency matrix $\mathbf{A}$ with entries $A_{ij} = 1$ if nodes i and j are connected by an edge and $A_{ij} = 0$ otherwise. Each node i's number of directly connected neighbors k_i is computed as $k_i = \sum_j A_{ij}$ and is referred to as the degree of node i. For this work, we further assume undirected networks with no self-loops. Thus, $\mathbf{A}=\mathbf{A}^{\mathrm{T}}$, $A_{ii} = 0 \; \forall \; i = 1, \ldots, N$, and $k_i \leqslant N - 1$.

Analogously to the concept of a *complexity-entropy plane* in nonlinear time series analysis, which has been utilized to discriminate between different types of time series generated by stochastic and deterministic chaotic processes [21,22], we aim to characterize a set of complex networks by means of its average per-node Shannon entropy S and a statistical complexity measure C. We thereby make use of two notions that are related with the complexity of a physical system, namely its *information content* and its state of *disequilibrium* [37–39]. In particular, we relate the information content of the network with the entropy S and the disequilibrium with the network's Jenson-Shannon divergence Q with respect to an appropriately chosen reference state.

Before going to the case of complex networks we discuss as a preliminary and as an analogy to classical statistical physics the two most extreme cases of complexity one might consider, namely the crystal as well as the ideal gas displaying a large and a low degree of order, respectively [37,40,41].

It is easily deductible that due to its regular structure, the crystal usually contains low or almost zero information, and, hence $S \to 0$. In contrast to this, the ideal gas (due to its disorder) contains a large amount of information, implying $S \gg 0$. Further, it is observed, that the perfect crystal displays among the highest disequilibrium ($Q \gg 0$), i.e., a large degree of order, while the ideal gas displays the exact opposite ($Q \to 0$). As both measures, S and Q, usually increase or decrease monotonically with a system's complexity, we ultimately derive a measure of statistical complexity C as the product of both information content (e.g., Shannon entropy S) and disequilibrium (e.g., Jenson-Shannon divergence Q) [37]. In the following we transfer the notion of information content and disequilibrium to the case of complex networks and derive corresponding terms for the entropy S and the statistical complexity C that then ultimately form the two-dimensional complexity-entropy plane.

A. Network entropy

Generally, the classical Shannon entropy for a discrete probability distribution P is given by

$$S(P) = -\sum_k p_k \log p_k. \tag{1}$$

Here p_k denotes the probability of occurrence for a given state k. Since averaged per-node entropies have been shown to generally serve as a good choice for discriminating between different types of networks [29], we choose here one specific definition of entropy that is based on the assessment of probabilities to jump between nodes when randomly traveling through the network and that has been successfully applied to the study of complex networks constructed from univariate time series [31]. In particular, the entropy S_i for each node i is computed based on the distribution P_i with entries $p_{i\to j}$ that give the uniformly distributed probability to jump from node i to node j along an edge between them in exactly one step. Thus, the corresponding random walk is formulated analogously to its application in computing the recently proposed *random-walk betweenness* [42]. If a node i is not fully disconnected from the rest of the network (i.e., $k_i > 0$), then the corresponding probabilities $p_{i\to j}$ are given by

$$p_{i\to j} = \frac{A_{ij}}{k_i} \in \{0, 1/k_i\} \tag{2}$$

with $\sum_j p_{i\to j} = 1$. The node entropy then reads

$$\begin{aligned} S_i(P_i) &= -\sum_{j=1}^{N} p_{i\to j} \log p_{i\to j} \\ &= -\sum_j \frac{A_{ij}}{k_i} \log \frac{A_{ij}}{k_i} = \log k_i. \end{aligned} \tag{3}$$

In case of an isolated node i with k_i=0, we set $S_i(P_i)$=0. Ultimately, the average normalized entropy taken over all nodes i is referred to as the network entropy,

$$S(P) = \frac{1}{N\log(N-1)} \sum_i S_i(P_i) \in [0,1]. \tag{4}$$

This specific definition of entropy is in accordance with some magnitude-based information indices [25] that measure tendencies for complex networks to form branches. In particular, our measure quantifies the heterogeneity in the network's degree distribution in a sense that nodes with low degree, i.e., peripheral nodes lower the overall network entropy $S(P)$ while high degree-hubs cause its increase. Thus, the present definition of $S(P)$ incorporates not only average statistics of the network's degree distribution but implicitly also accounts for its higher moments, such as the variance.

The entropy $S(P)$ can further be interpreted with respect to the underlying formulation of the random walk. In the limiting case of a fully connected network the probability to jump between nodes is given as $p_{i\to j} = \frac{1}{N-1}\ \forall\ i \neq j$. Thus, the walk becomes fully random in a sense that no node j is excluded as a possible candidate for the walker to jump to. This case is directly related to the notion of the ideal gas outlined above where all micro states are equally probable and, thus, the entropy is maximized. Analogously, for the fully connected network all walks through the network of arbitrary length are equally probable, too. Consequently, the entropy $S(P)$ is also maximized and reads $S(P) = 1$.

In turn, for a sparsely connected network the jumps of the walker become more deterministic and in the limiting case of, e.g., node i only having one neighbor n, its associated traverse probabilities approach $p_{i\to j} = \delta_{jn}$ (with δ_{jn} being Kronecker's delta). In this case, the walker has only one option for jumping to a neighboring node of i. Consequently, the entropy is lowered and for sufficiently sparse networks approaches $S(P) \to 0$. Again, this case may be interpreted in analogy to a regular crystal that displays perfect order as well as a deterministic structure and, hence, has a low information content.

In summary, we thus interpret our definition of $S(P)$ as a measure of regularity or order in the network under study with respect to its navigability that is measured in terms of a random walk.

B. Statistical complexity

We aim to express statistical complexity or nontriviality in terms of a system's disequilibrium and information content [37], with the latter being defined as the network entropy $S(P)$ that is introduced above. Along the lines of common statistical mechanics, disequilibrium is conveniently measured in terms of the (per-node) Jenson-Shannon divergence [43]

$$\begin{aligned} Q_i(P_i, P_{i,e}) = Q_0\{&S_i(0.5[P_i + P_{e,i}]) \\ &- 0.5[S_i(P_i) + S_i(P_{e,i})]\}, \end{aligned} \tag{5}$$

with $Q_0 = 1/\log 2$ to ensure $Q_i \in [0,1]$. This metric takes low values for systems that are close to equilibrium like an ideal gas and high values for systems in disequilibrium like the perfect crystal. Here the probability distribution P_i with entries as introduced in Eq. (2) again denotes the probabilities to jump between neighboring nodes i and j when randomly traveling through the network. The distribution $P_{e,i}$ denotes the same but for an appropriately chosen reference or equilibrium state, i.e., network. Analogously to previous works, we assume that a system is in equilibrium if its state corresponds to the fully randomized one [43]. For the case of complex networks, this equilibrium state would than be a corresponding Erdős-Rényi [44] random network. We introduce the specific details of this choice in Sec. II C.

Analogously to the network entropy, the Jenson-Shannon divergence Q of the entire network is again computed as the arithmetic mean of all per-node values Q_i,

$$Q(P, P_e) = \frac{1}{N} \sum_i Q_i(P_i, P_{i,e}). \tag{6}$$

As for the case of the network entropy $S(P)$, the analogy with generic physical systems (perfect crystal and ideal gas) is apparent.

Again, the fully connected network corresponds to the case of an ideal gas with minimum disequilibrium as any appropriately chosen reference network should be fully connected as well, which implies $P = P_e$ and, thus, $Q = 0$. In contrast, a randomly chosen reference to a sparsely connected network most certainly displays a different microscopic structure. Hence, the probabilities P and P_e for jumping between nodes also differ, yielding a high disequilibrium $Q \gg 0$.

With the above observations in mind, we demand based on common sense that neither the fully connected nor the very sparsely connected (or almost empty) network should be attributed a large complexity. Hence, neither a measure of *information* [$S(P)$] nor *disequilibrium* [$Q(P, P_e)$] alone may serve as an appropriate quantifier of statistical complexity. However, a measure of statistical complexity C has been proposed that is based on a product of the two quantities [21,37],

$$C(P) = Q(P, P_e)S(P) \in [0,1]. \tag{7}$$

This measure intuitively exhibits the required asymptotic properties, such that for the limiting case $S(P) = 0$, it follows that $C(P) = 0$. Analogously, $S(P) = 1$ is only achieved for a fully connected network which implies $P = P_e$ (see Sec. II C for details) and $Q(P, P_e) = 0$, which also yields $C(P) = 0$. For all cases $0 < S(P) < 1$, the statistical complexity $C(P)$ has a possible upper bound that is determined by $S(P)$. However, its analytical expression has so far only been obtained for a binary state probability distribution [39].

We ultimately note that a variety of further measures has been developed that similarly aim to quantify complexity in dynamical systems [45]. However, most of these measures are more tailored to other applications, such as the numerical detection of bifurcations, e.g., order–chaos or chaos–chaos transitions. We thus focus in this work on the statistical complexity measure as introduced above.

C. Reference networks

In order to compute the Jenson-Shannon divergences Q_i and Q we need to compare each network's set of probability distributions P_i to jump between a node i and its neighbors

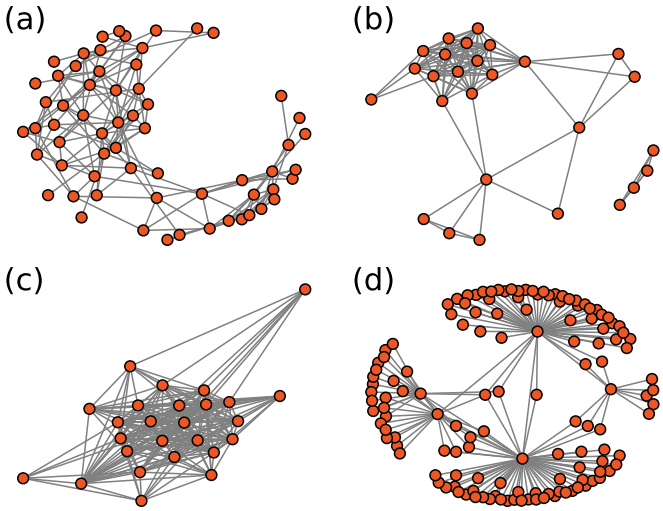

FIG. 1. Selection of 4 of the 29 networks investigated in this study: Dolphin (a), zebra (b), and bison (c) animal social networks as well as the network of American revolutionary groups (d).

with an appropriately chosen baseline or equilibrium $P_{i,e}$. We note here that defining the equilibrium state of a network is a highly nontrivial task that is often achieved by fitting the network under study to a certain network model using numerical variational techniques in order to minimize or maximize a target or cost function [46,47]. However, in order to demonstrate the applicability of our approach and to focus on the numerical properties of the statistical complexity C, we chose to define the equilibrium or reference state of a given network as its fully randomized counterpart and, thus, interpret C as an indicator of statistical independence from a corresponding random state. In this case, one obvious candidate for such a baseline network is the Erdős-Rényi random graph [44]. To account for the stochasticity of this model, we generate for each network under study an ensemble of $n = 100$ independent Erdős-Rényi networks with the same number of nodes N and linking probability $\rho = \sum_i k_i/[N(N-1)]$ and compute ensemble average quantities of Q_i, Q and C from the resulting probability distributions $P_{i,e}$.

D. Real-world networks

We study the entropy S and statistical complexity C of 29 real-world networks, for which we assign types according to their sub-domains in the Colorado Index of Complex Networks (ICON) (https://icon.colorado.edu/). Specifically, we study 8 networks that represent social networks among different species of animals, 5 transportation networks, 4 networks representing affiliations between people or corporations, and 12 connectome networks for different species. In order to make the results comparable, we treat all networks under study as being unweighted, undirected, and without self-loops. The networks under study, together with their assigned type, number of nodes N, and link density ρ are summarized in Table I. Visual representations of the topological structure of 4 of the 29 networks are shown in Fig. 1. The network parameters N and ρ will be used to compute corresponding reference networks as outlined in Sec. II C.

E. Threshold-based networks

In addition to real-world networks, we aim to illustrate the usefulness of the statistical complexity C as a measure to objectively construct threshold-based networks. Generally, these types of networks are constructed from $N \times N$ matrices that describe some spatial or similarity relationship between nodes [73].

We first study one prototypical example of a threshold-based network in terms of a recurrence network [36,74] constructed from the three-dimensional Rössler system given by

$$\frac{dx}{dt} = -y - z, \tag{8}$$

$$\frac{dy}{dt} = x + ay, \tag{9}$$

$$\frac{dz}{dt} = b + z(x - c). \tag{10}$$

We set $a = b = 0.2$ and $c = 5.7$ as in the original study of this system [75]. In the past, recurrence networks have been shown to capture essential information on the phase space structure of the dynamical system under study and thus serve as a good (or even equivalent) representation of the system's trajectory [76,77]. Each node i in the network represents a point $\vec{x}_i = (x(t_i), y(t_i), z(t_i))$ on the system's trajectory at randomly chosen times $t_i \in [100, 1000]$, where $t_i \geqslant 100$ ensures that for our choice of initial values $x(0) = y(0) = z(0) = 1$ the system has converged onto the chaotic attractor. The entries D_{ij} of the distance matrix $\mathbf{D}$ are then given by the Euclidean distances between points $\vec{x}_i$ and $\vec{x}_j$ [36]. From $\mathbf{D}$, a corresponding recurrence matrix $\mathbf{R}$ with entries R_{ij} is constructed by choosing a recurrence threshold T such that

$$R_{ij} = \Theta(T - D_{ij}), \tag{11}$$

where $\Theta(\cdot)$ denotes the Heaviside function. $\mathbf{R}$ is now interpreted as the adjacency matrix of a spatial recurrence network such that $A_{ij} = R_{ij} - \delta_{ij}$. Hence, only distances between points that are smaller than a critical distance T are connected in the resulting network. The threshold T is chosen such that a desired link density or *recurrence rate* ρ is obtained.

Another case of threshold-based networks are functional networks. Here, a similarity matrix $\mathbf{M}$ is constructed from pairwise statistical interdependencies between time series that are represented by nodes in the network. These nodes may correspond to different channels of electroencephalography (EEG) signals in neural networks [7] or records of climatic variables at different locations of the Earth in so-called climate networks [34,35]. Specifically, the latter have been shown to encode valuable information on the large-scale dynamical organization of spatially extended components of the climate system, such as ocean currents [78] or the El Niño Southern Oscillation [79]. As an example for such functional climate networks, we compute the pairwise Pearson correlation between all $N = 10,224$ time series of (i) monthly averaged surface air temperature and (ii) monthly averaged sea level pressure from the NCEP/NCAR 40-year reanalysis project [80] that is provided by the National Center of Oceanic and Atmospheric Research. Analogously to Eq. (11), a threshold is applied to the thus obtained similarity matrix

TABLE I. Overview of the networks evaluated in this study together with their respective number of nodes N and link density ρ as well as entropy S and statistical complexity C computed over an ensemble of $n = 100$ reference networks. The provided estimate of the error in C denotes one standard deviation. Categories have been assigned according to their classification in the Colorado Index of Complex Networks (ICON) (https://icon.colorado.edu/).

Name	Category	N	ρ	S	C
Sheep [48]	Social Animal	28	0.622	0.825	0.326 ± 0.022
Rhesus [49]	Social Animal	16	0.575	0.753	0.341 ± 0.035
Kangaroo [50]	Social Animal	17	0.669	0.782	0.285 ± 0.024
Mac [51]	Social Animal	62	0.617	0.874	0.339 ± 0.009
Bison [52]	Social Animal	26	0.683	0.855	0.281 ± 0.019
Zebra [53]	Social Animal	27	0.316	0.571	0.409 ± 0.024
Cattle [54]	Social Animal	28	0.542	0.772	0.372 ± 0.018
Dolphins [55]	Social Animal	62	0.084	0.342	0.317 ± 0.006
Autobahn [5]	Transportation	1,168	0.002	0.099	0.099 ± 0.000
USairport500 [56]	Transportation	500	0.024	0.250	0.246 ± 0.001
USairport 2010 [57]	Transportation	1,574	0.014	0.248	0.246 ± 0.000
Openflights [57]	Transportation	2,939	0.004	0.173	0.173 ± 0.000
Rome99 [58]	Transportation	3,353	0.001	0.121	0.121 ± 0.000
South-Africa [59]	Social Affiliation	6	0.633	0.601	0.306 ± 0.062
American Revolution [60]	Social Affiliation	136	0.017	0.043	0.043 ± 0.001
Club-Membership [61]	Social Affiliation	25	0.305	0.576	0.415 ± 0.021
Corporate-Leadership [62]	Social Affiliation	24	0.322	0.590	0.417 ± 0.026
Rhesus Brain 1 [63]	Connectome	242	0.105	0.523	0.474 ± 0.002
Rhesus Brain 2 [64]	Connectome	91	0.142	0.452	0.401 ± 0.006
Mouse Retina 1 [65]	Connectome	1,076	0.157	0.693	0.594 ± 0.001
Mixed Species Brain 1 [66]	Connectome	65	0.351	0.717	0.478 ± 0.012
Rhesus Cerebral Cortex 1 [67]	Connectome	91	0.342	0.710	0.485 ± 0.007
C Elegans Neural Male 1 [68]	Connectome	269	0.081	0.486	0.451 ± 0.002
Rattus Norvegicus Brain 3 [69]	Connectome	493	0.214	0.684	0.558 ± 0.001
Rhesus Interareal Cortical Network 2 [70]	Connectome	93	0.529	0.822	0.413 ± 0.006
Rattus Norvegicus Brain 2 [69]	Connectome	502	0.196	0.666	0.556 ± 0.001
Rattus Norvegicus Brain 1 [69]	Connectome	503	0.182	0.653	0.553 ± 0.001
Mouse Brain 1 [71]	Connectome	213	0.716	0.934	0.272 ± 0.003
C Elegans Herm Pharynx 1 [72]	Connectome	279	0.059	0.460	0.436 ± 0.002

M (containing the absolute values of the pairwise Pearson correlations, i.e., $M_{ij} = |C_{ij}|$), such that only a certain fraction of the largest values are considered as links in the resulting network. Therefore,

$$A_{ij} = \Theta(M_{ij} - T) \cdot (1 - \delta_{ij}), \tag{12}$$

with A_{ij} being the entries of the resulting adjacency matrix **A**. Again, the threshold T is usually chosen such that a desired network link density ρ is achieved.

III. RESULTS

We now study in a first application the numerical values of entropy S and complexity C for the different real-world networks. To further consolidate our findings we then also study two different classes of synthetic networks, namely Watts-Strogatz networks with different rewiring probabilities [13] and random scale-free networks with a prescribed exponent of the power-law degree distribution. Ultimately, in a last use case, we illustrate the application of statistical complexity to objectively determine appropriate thresholds for the construction of threshold-based networks.

A. Real-world networks

Figure 2(a) displays the entropy S and average statistical complexity C of all real-world networks under study with respect to ensembles of $n = 100$ Erdős-Rényi reference networks that reflect the original networks' respective properties (the average numerical values of S and C are also presented in Table I). In addition, error bars indicate the corresponding standard deviation taken over all ensemble members and are shown when their size exceeds that of the corresponding symbol. For reference, we also compute and display the complexity and entropy of a set of 50 Erdős-Rényi networks with the number of nodes N and linking probability ρ drawn uniformly at random from the intervals [10,1000] and (0,1], respectively [Fig. 2].

We note that the different types of networks under study generally occupy distinct areas in the complexity-entropy plane [Fig. 2(a)]. While connectome networks show among the highest values of C, we note intermediate values for both types of social networks and the lowest values for the transportation networks. Additionally, the latter also exhibit among the lowest values of entropy S. Notable exceptions are the social networks of dolphins and zebras, which in contrast to most of the other animal networks display a unique community structure [see Figs. 1(a) and 1(b) for a visual representation].

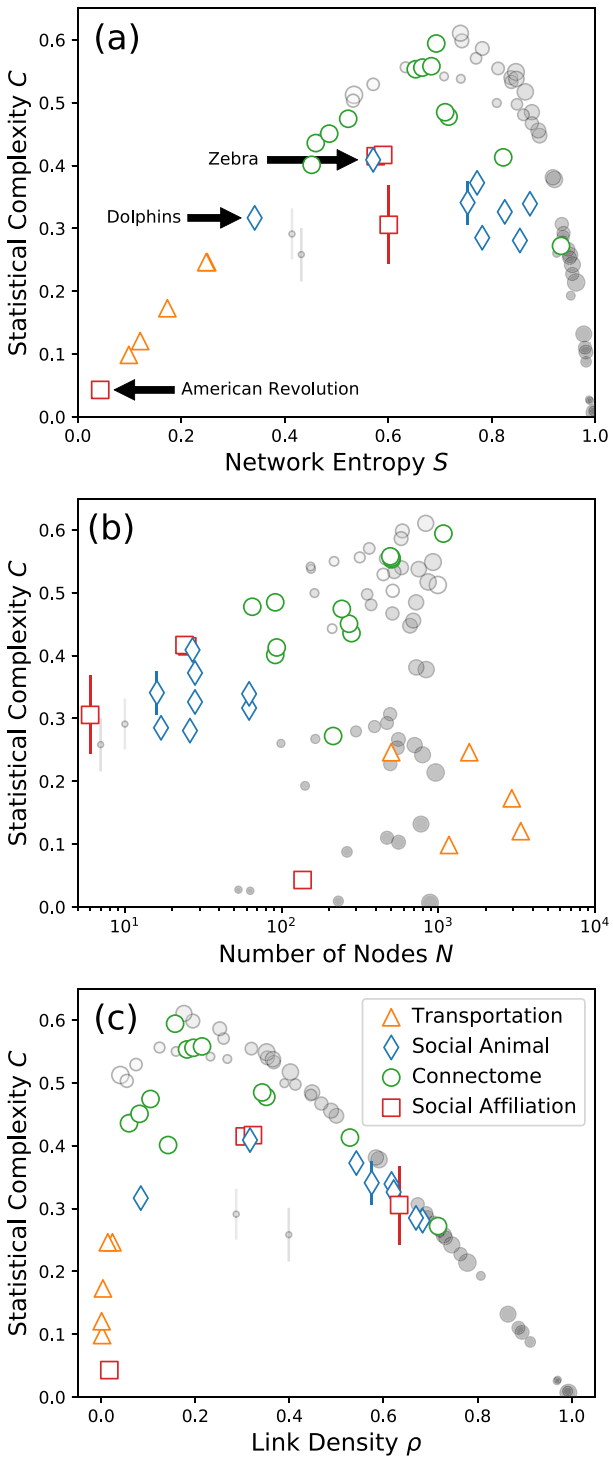

FIG. 2. (a) Mapping of real-world networks in the complexity-entropy plane. Additionally, gray scatter show the results for 50 different Erdős-Rényi random networks. Here, the size and transparency denotes the uniformly at random drawn number of nodes N from the interval $[10,1000]$ and linking probability ρ from the interval $(0,1]$, respectively. (b) Dependence of the statistical complexity C on the number of nodes N in each network under study. (c) The same as in (b) for the link density ρ. Error bars indicate one standard deviation of statistical complexity taken over the ensemble of $n = 100$ random Erdős-Rényi reference networks with respect to the corresponding real-world network under study and are shown if their size exceeds that of the corresponding symbol.

Specifically, the dolphin network [Fig. 1(a)] is characterized by two distinct communities that are connected only via few nodes while the zebra network [Fig. 1(b)] is composed of one large almost fully connected community containing roughly half of the nodes and at least two further distinct communities with only few nodes that hardly connect with the main herd. In contrast, all the other animal networks [see Fig. 1(c) for a representative example] generally display a similar structure with only one densely connected community. Another outstanding exception is the network of American revolutionary groups [Fig. 1(d)], which due to its distinct hierarchical structure displays very low values of entropy and complexity. We conclude from these first observations that the complexity-entropy plane generally distinguishes well between different types of networks solely based on their specific and distinct topology.

For the random Erdős-Rényi networks (gray symbols in Fig. 2) we find that in many cases they show a higher statistical complexity than real-world networks. In fact, their values roughly seem to determine an upper bound of C for each possible value of S [Fig. 2(a)]. This behavior is expected, as the two networks that are compared in the Jenson-Shannon divergence $Q(P, P_e)$, the Erdős-Rényi network under study and a random reference network, are statistically fully independent by construction and, more importantly, therefore less or equally statistically dependent than any real-world complex network in comparison with a random reference network. However, we note that this property only seems to hold for sufficiently large networks [Fig. 2(a)].

Since the topological characteristics of the Erdős-Rényi network only depend on the given number of nodes N and linking probability or link density ρ, we examine the dependence of C on both parameters individually. Figure 2(b) shows the values of statistical complexity C as a function of the number of nodes N in each network which displays no clear dependence between the two variables. In contrast, a possible dependence between link density ρ and statistical complexity C is observed [Fig. 2(c)]. Still, we note that networks with highly dissimilar link densities ρ may exhibit similar statistical complexity [Fig. 2(c)].

Furthermore, the quantitatively similar functional dependencies between S and C [Fig. 2(a)] as well as ρ and C imply an expected functional dependence between S and ρ. However, the S-C plane is a much better choice for categorizing networks than the ρ-C plane since the entropy S captures all moments in the degree distribution of a given network [as can be seen from the series expansion of $\sum_i \log k_i$ in Eq. (4)], while ρ only captures its first moment.

B. Synthetic networks

To further consolidate the above findings we now systematically study numerically the statistical complexity C for two different types of synthetic networks, i.e., random scale-free and Watts-Strogatz networks. Figure 3(a) shows the statistical complexity C averaged over an ensemble of $n = 50$ random scale-free networks with power-law-shaped degree distributions at different exponents α and different numbers of nodes $N = 2500$, $N = 5000$, and $N = 10,000$. Here, each individual scale-free network is compared to one realization of

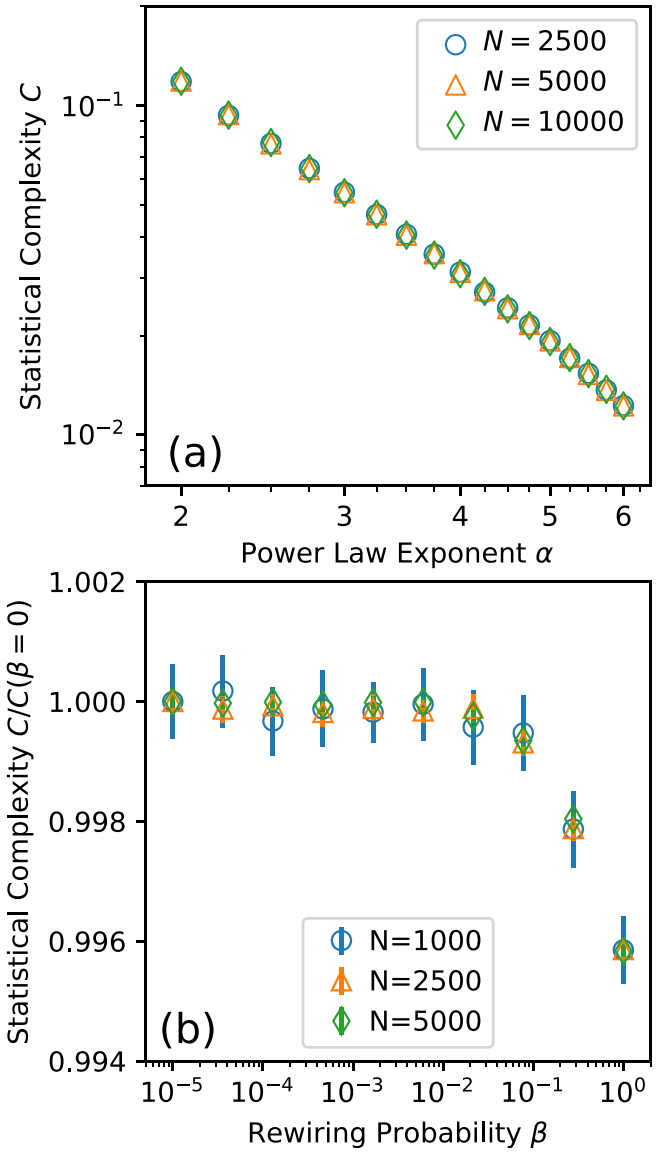

FIG. 3. (a) Average statistical complexity C for different power-law exponents α in the degree distribution of randomly generated scale-free networks. Each scatter denotes the average over an ensemble of 50 networks consisting of $N = 2500$, $N = 5000$ and $N = 10{,}000$ nodes, respectively. (b) The same for different choices of the rewiring probability β in the Watts-Strogatz model with an average degree of $K = 20$. For comparison all average statistical complexities are rescaled by $C(\beta = 0)$ of the regular ring graph. Error bars denote one standard deviation in the respective statistical complexity and are shown if their size exceeds that of the corresponding symbol.

a corresponding random reference network. In particular, the scale-free networks are constructed by first generating a degree sequence with a power-law-shaped distribution according to the considered power-law exponent α. Then, each network is created by iteratively inserting links between nodes according to the configuration model [1,2]. Ultimately, self-loops and multiple links are again excluded from the assessment. We observe a decrease in statistical complexity C with increasing α [Fig. 3(a)]. For small values of α the networks display a heterogeneous degree distribution with the presence of both hubs and peripheral nodes. Consequently, the statistical complexity C takes comparatively large values. In contrast, for high values of α the networks become increasingly sparse with only few links present per node and, thus, they display a narrower degree distribution. In this case the distinction between hubs and peripheral nodes is less apparent and the network itself may be considered less statistically complex which manifests in comparably low values of C. We also note that due to the scale-free property of the considered networks the statistical complexity C seems to be independent of the number of nodes N [Fig. 3(a)].

As a second family of model networks we study the statistical complexity C for an ensemble of networks constructed from the Watts-Strogatz model for different choices of the rewiring probability β. Again, we construct networks of different sizes with $N = 1000$, $N = 2500$, and $N = 5000$ nodes and a fixed average degree of $K = 20$. Starting from a ring graph where every node has $K/2$ left and right neighbors, each link in the network is rewired with probability β. As above, we obtain for each choice of N and β an ensemble of $n = 50$ randomly generated networks and compute the corresponding statistical complexity C by again comparing each ensemble member with one realization of a corresponding Erdős-Rényi random network and averaging the obtained results [Fig. 3(b)]. In order to render the results comparable, we rescale all obtained values by the corresponding statistical complexity of the ring graph with $\beta = 0$. The corresponding values of this rescaling-factor read $C(\beta = 0) = 0.425$ for $N = 1000$, $C(\beta = 0) = 0.380$ for $N = 2{,}500$, and $C(\beta = 0) = 0.350$ for $N = 5000$, respectively. Thus, C decreases with increasing N as the networks become more sparse. In contrast to the above case of scale-free networks we note only minor, yet systematic, changes of C with varying β [Fig. 3(b)]. In particular, the observed drop in statistical complexity occurs for values of the rewiring probability between $\beta = 0.01$ and $\beta = 0.1$. These values coincide with the onset of the transition between small-world and random network structure in the Watts-Strogatz model [13].

The observed small variations in C may be explained from the underlying definition of the statistical complexity as a result of a random walk between nodes in the network. Rewiring the network structure of a ring graph only induces minor changes to its degree distribution, i.e., from a single peak at the average degree K for $\beta = 0$ to approximately a Poisson distribution centered around K for $\beta = 1$. Since the random walk is to a large extent determined by the functional form of this underlying distribution, resulting values of C consequently vary only little with β. Ultimately, we note that by rescaling the obtained values of C with corresponding values of the ring graph, the relative changes in C with varying β are largely similar for all choices of N.

C. Threshold-based networks

We now turn our focus to the threshold-based networks introduced in Sec. II E. Figure 4 shows the statistical complexity C of three recurrence networks with $N = 2500$, $N = 5000$, and $N = 10{,}000$ nodes obtained from the Rössler system [Eqs. (8)–(10)] depending on the link density ρ that is applied to obtain the recurrence matrix $\mathbf{R}$ [Eq. (11)]. For all cases, C

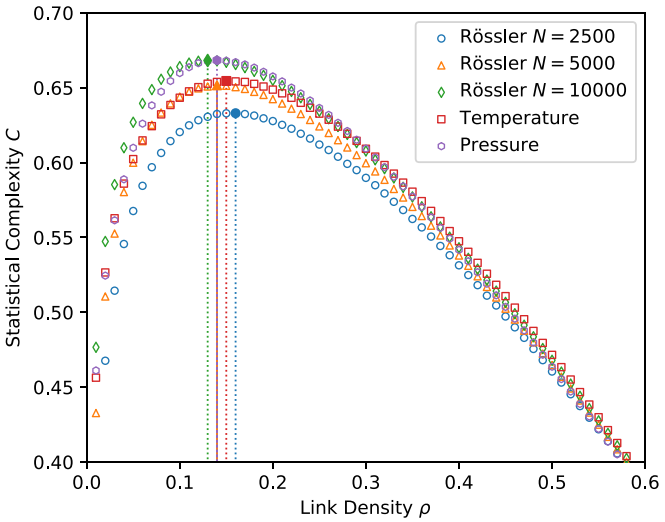

FIG. 4. Statistical complexity C depending on the threshold-based networks' link densities ρ for three recurrence networks with different numbers of nodes N constructed from the Rössler system and two functional climate networks representing surface air temperature and sea level pressure variations, respectively. Filled symbols denote the maximum value of statistical complexity for each network. Dotted lines indicate the corresponding link density $\rho_{\max}$, which maximizes the statistical complexity. No error bars are shown as the standard deviation of C taken over all $n = 100$ reference networks is always smaller than the size of the symbols.

is computed as the average statistical complexity taken over an ensemble of $n = 100$ reference networks.

We note that C increases with increasing ρ until a maximum is reached at $\rho_{\max} = 0.16$, $\rho_{\max} = 0.14$ and $\rho_{\max} = 0.13$ for $N = 2500$, $N = 5000$, and $N = 10{,}000$, respectively (Fig. 4). For values $\rho > \rho_{\max}$ the statistical complexity decreases monotonically and approaches $C = 0$ for $\rho = 1$ (not shown). Usually, when constructing recurrence networks a link density of order $\mathcal{O}(10^{-2})$ is chosen heuristically, even though it was suggested that with such comparably low choices of recurrence rates possibly significant interdependencies between nodes might be suppressed [36,81,82]. Our results indicate that larger choices of recurrence rates and corresponding thresholds T might yield a recurrence network with higher statistical complexity and, thus, a larger degree of nontrivial structure than the ones that were previously typically studied.

For the functional networks that are constructed from climate time series across the globe according to Eq. (12) at different link densities ρ, we find that the link densities that are maximizing the statistical complexity are $\rho_{\max} = 0.15$ and $\rho_{\max} = 0.14$ for the temperature and pressure field, respectively. As for the recurrence network studied above, these values are again considerably larger then the usually employed link densities of order $\mathcal{O}(10^{-2})$ [35,78]. However, it has again been reported that these usually employed small choices of link density and the corresponding high threshold may suppress statistically significant signals associated with comparably lower pairwise similarity values [83]. Thus, future work in this area could apply our formalism to determine a more objectively chosen threshold than in previous studies.

We emphasize that even though we only present two different use cases as examples, our framework may be applicable to any kind of functional network that is constructed from some pairwise functional interdependencies between nodes, including neural [7,69] or economic networks [84]. Beyond this, our framework might also be applicable to networks constructed from non-pair-wise interdependencies that are investigated in, e.g., causal effect networks [74,85,86]. The assessment of statistical complexity could help to more objectively choose thresholds for the construction of such networks and complements existing approaches based on, e.g., the assessment of the recurrence network's percolation threshold [76,87,88].

IV. CONCLUSION AND OUTLOOK

We have presented a methodology to categorize complex networks by means of an entropy measure and an estimator of statistical complexity. In particular, our method computes for each network under study an average per-node Shannon entropy that is based on probabilities to randomly jump between neighboring nodes in the network. From this, we estimate a network's statistical complexity by computing the Jenson-Shannon divergence between a given network and a set of corresponding Erdős-Rényi random networks. We find that networks of different types, such as social or infrastructure networks, generally occupy distinct regions in the two-dimensional complexity-entropy plane and our proposed framework thus discriminates well between them. Moreover, we find that connectome networks are among the statistically most complex ones while infrastructure networks generally display a lower complexity. These properties might intuitively be expected when considering the term complexity with respect to real-world structures and the associated functions thereof.

We have further shown in a second application that the notion of statistical complexity can be applied to objectively estimate thresholds for the construction of functional networks, such that a network's statistical complexity is maximized and, hence, contains most non-trivial information.

Starting from the demonstrated possible scenarios for applying the proposed methodology, future work should investigate in more detail the discriminating power of the statistical complexity for a broader set of real-world complex networks. In particular, as we have observed that within our framework connectome networks are among the most complex ones, we suggest to further investigate the interplay between the statistical complexity and the complexity of structure-function relations in such networks [89] in future work. Additionally, the framework should be generalized to the case of weighted and/or directed networks. For this purpose, more emphasis must be put into the definition of the reference networks, which for now have been assumed to just be a randomized correspondent of the specific network under study. Another interesting line of inquiry would be to study the dependence of the statistical complexity with respect to the choice of the underlying random walk, such as the maximum entropy random walk [90], as an alternative to the generic one-step random walked used in this paper.

In general, our framework expands the understanding of complex topological structures and helps to quantify varying

degrees of complexity in various systems. Our approach should be useful for many disciplines of (applied) complex network science, such as neuro-, social, or even climate science.

ACKNOWLEDGMENTS

M.W. and R.V.D. have been supported by the German Federal Ministry for Education and Research (BMBF) via the Young Investigators Group CoSy-CC^2 (Grant No. 01LN1306A). J.F.D. thanks the Stordalen Foundation via PB.net and the Earth League's EarthDoc program. M.W. and J.F.D. thank the Leibniz Association (project DOMINOES) for financial support. J.K. and R.V.D. acknowledge the IRTG 1740 funded by DFG and FAPESP. The authors thank Jobst Heitzig and Michael Small for fruitful discussions in the course of conducting this study. The European Regional Development Fund (ERDF), the German Federal Ministry of Education and Research, and the Land Brandenburg have greatly supported this project by providing resources on the high performance computer system at the Potsdam Institute for Climate Impact Research.

[1] S. Boccaletti, V. Latora, Y. Moreno, M. Chavez, and D. Hwang, Phys. Rep. **424**, 175 (2006).
[2] M. E. J. Newman, SIAM Rev. **45**, 167 (2003).
[3] D. P. Croft, R. James, and J. Krause, *Exploring Animal Social Networks* (Princeton University Press, Princeton, NJ, 2008).
[4] P. K. McGregor, *Animal Communication Networks* (Cambridge University Press, Cambridge, UK, 2005).
[5] M. Kaiser and C. C. Hilgetag, Phys. Rev. E **69**, 036103 (2004).
[6] M. T. Gastner and M. E. J. Newman, Eur. Phys. J. B **49**, 247 (2006).
[7] E. Bullmore and O. Sporns, Nat. Rev. Neurosci. **10**, 186 (2009).
[8] O. Sporns, G. Tononi, and R. Kötter, PLoS Comput. Biol. **1**, e42 (2005).
[9] R. Albert and A.-L. Barabási, Rev. Mod. Phys. **74**, 47 (2002).
[10] M. Barthélemy, Phys. Rep. **499**, 1 (2011).
[11] M. Dehmer and A. Mowshowitz, Inform. Sci. **181**, 57 (2011).
[12] L. d. F. Costa, F. A. Rodrigues, G. Travieso, and P. R. Villas Boas, Adv. Phys. **56**, 167 (2007).
[13] D. J. Watts and S. H. Strogatz, Nature **393**, 440 (1998).
[14] K.-I. Goh, E. Oh, H. Jeong, B. Kahng, and D. Kim, Proc. Natl. Acad. Sci. USA **99**, 12583 (2002).
[15] M. Wiedermann, J. F. Donges, J. Kurths, and R. V. Donner, Phys. Rev. E **93**, 042308 (2016).
[16] R. Milo, S. Itzkovitz, N. Kashtan, R. Levitt, S. Shen-Orr, I. Ayzenshtat, M. Sheffer, and U. Alon, Science **303**, 1538 (2004).
[17] A. Lancichinetti, M. Kivelä, J. Saramäki, and S. Fortunato, PLoS ONE **5**, e11976 (2010).
[18] K. Anand and G. Bianconi, Phys. Rev. E **80**, 045102(R) (2009).
[19] D. Bonchev and G. A. Buck, in *Complexity in Chemistry, Biology, and Ecology* (Springer, New York, 2005), pp. 191–235.
[20] M. Dehmer, N. Barbarini, K. Varmuza, and A. Graber, PLoS ONE **4**, e8057 (2009).
[21] O. A. Rosso, H. A. Larrondo, M. T. Martin, A. Plastino, and M. A. Fuentes, Phys. Rev. Lett. **99**, 154102 (2007).
[22] M. Martin, A. Plastino, and O. Rosso, Physica A **369**, 439 (2006).
[23] H. Lange, O. A. Rosso, and M. Hauhs, Eur. Phys. J. St. **222**, 535 (2013).
[24] N. Rashevsky, B. Math. Biophys. **17**, 229 (1955).
[25] D. Bonchev, *Information Theoretic Indices for Characterization of Chemical Structures* (Research Studies Press, Somerset, NJ, 1983), Vol. 5.
[26] R. F. I. Cancho and R. V. Solé, in *Statistical Mechanics of Complex Networks*, edited by R. Pastor-Satorras, M. Rubi, and A. Diaz-Guilera, Lecture Notes in Physics No. 625 (Springer, Berlin, 2003), pp. 114–126.
[27] B. Wang, H. Tang, C. Guo, and Z. Xiu, Physica A **363**, 591 (2006).
[28] G. Bianconi, Europhys. Lett. **81**, 28005 (2008).
[29] M. Dehmer, M. Grabner, and K. Varmuza, PLoS ONE **7**, e31214 (2012).
[30] E. V. Konstantinova, V. A. Skorobogatov, and M. V. Vidyuk, Ind. J. Chem. A **42A**, 1227 (2003).
[31] M. Small, in *2013 IEEE International Symposium on Circuits and Systems (ISCAS)* (IEEE, Los Alamitos, CA, 2013), pp. 2509–2512.
[32] L. A. Amaral and J. M. Ottino, Eur. Phys. J. B **38**, 147 (2004).
[33] D. R. White and M. Houseman, Complexity **8**, 72 (2002).
[34] A. A. Tsonis, K. L. Swanson, and P. J. Roebber, Bull. Am. Meteorol. Soc. **87**, 585 (2006).
[35] J. F. Donges, Y. Zou, N. Marwan, and J. Kurths, Eur. Phys. J. St. **174**, 157 (2009).
[36] R. V. Donner, Y. Zou, J. F. Donges, N. Marwan, and J. Kurths, New J. Phys. **12**, 033025 (2010).
[37] R. López-Ruiz, H. L. Mancini, and X. Calbet, Phys. Lett. A **209**, 321 (1995).
[38] X. Calbet and R. López-Ruiz, Phys. Rev. E **63**, 066116 (2001).
[39] P. W. Lamberti, M. T. Martin, A. Plastino, and O. A. Rosso, Physica A **334**, 119 (2004).
[40] P. W. Anderson, Phys. Today **44**, 9 (1991).
[41] G. Parisi, Phys. World **6**, 42 (1993).
[42] M. E. J. Newman, Soc. Networks **27**, 39 (2005).
[43] M. Martin, A. Plastino, and O. Rosso, Phys. Lett. A **311**, 126 (2003).
[44] P. Erdős and A. Rényi, Publ. Math. Inst. Hung. Acad. Sci **5**, 17 (1960).
[45] R. Wackerbauer, A. Witt, H. Atmanspacher, J. Kurths, and H. Scheingraber, Chaos Soliton. Fract. **4**, 133 (1994).
[46] S. Dafermos and A. Nagurney, Math. Prog. **28**, 174 (1984).
[47] F. Giannessi and A. Maugeri (eds.), *Variational Inequalities and Network Equilibrium Problems* (Springer, Boston, MA, 1995).
[48] C. C. Hass, J. Zool. **225**, 509 (1991).
[49] D. S. Sade, Folia Primatol. **18**, 196 (2004).
[50] T. R. Grant, Anim. Behav. **21**, 449 (1973).
[51] L. M. Fedigan and P. J. Asquith, *The Monkeys of Arashiyama: Thirty-Five Years of Research in Japan and the West* (SUNY Press, Albany, NY, 1991).
[52] D. F. Lott, Z. Tierpsychol. **49**, 418 (1979).
[53] S. R. Sundaresan, I. R. Fischhoff, J. Dushoff, and D. I. Rubenstein, Oecologia **151**, 140 (2007).
[54] M. W. Schein and M. H. Fohrman, Br. J. Anim. Beh. **3**, 45 (1955).

[55] D. Lusseau, K. Schneider, O. J. Boisseau, P. Haase, E. Slooten, and S. M. Dawson, Behav. Ecol. Sociobiol. **54**, 396 (2003).
[56] V. Colizza, R. Pastor-Satorras, and A. Vespignani, Nat. Phys. **3**, 276 (2007).
[57] www.toreopsahl.com/2011/08/12/
[58] www.dis.uniroma1.it/challenge9
[59] J. A. Hobson, *The Evolution of Modern Captitalism: A Study of Machine Production* (Scribners, New York, 1906).
[60] www.konect.uni-koblenz.de/networks/brunson_revolution
[61] K. Faust, Soc. Networks **19**, 157 (1997).
[62] R. Barnes and T. Burkett, Connections **30**, 4 (2010).
[63] L. Harriger, M. P. v. d. Heuvel, and O. Sporns, PLoS ONE **7**, e46497 (2012).
[64] N. T. Markov, J. Vezoli, P. Chameau, A. Falchier, R. Quilodran, C. Huissoud, C. Lamy, P. Misery, P. Giroud, S. Ullman, P. Barone, C. Dehay, K. Knoblauch, and H. Kennedy, J. Comp. Neurol. **522**, 225 (2014).
[65] M. Helmstaedter, K. L. Briggman, S. C. Turaga, V. Jain, H. S. Seung, and W. Denk, Nature **500**, 168 (2013).
[66] M. A. de Reus and M. P. van den Heuvel, J. Neurosci. **33**, 12929 (2013).
[67] N. T. Markov, M. M. Ercsey-Ravasz, A. R. R. Gomes, C. Lamy, L. Magrou, J. Vezoli, P. Misery, A. Falchier, R. Quilodran, M. A. Gariel, J. Sallet, R. Gamanut, C. Huissoud, S. Clavagnier, P. Giroud, D. Sappey-Marinier, P. Barone, C. Dehay, Z. Toroczkai, K. Knoblauch, D. C. van Essen, and H. Kennedy, Cereb. Cortex **24**, 17 (2014).
[68] T. A. Jarrell, Y. Wang, A. E. Bloniarz, C. A. Brittin, M. Xu, J. N. Thomson, D. G. Albertson, D. H. Hall, and S. W. Emmons, Science **337**, 437 (2012).
[69] M. Bota and L. W. Swanson, J. Comp. Neurol. **500**, 807 (2007).
[70] N. T. Markov, M. M. Ercsey-Ravasz, C. Lamy, A. R. R. Gomes, L. Magrou, P. Misery, P. Giroud, P. Barone, C. Dehay, Z. Toroczkai, K. Knoblauch, D. C. van Essen, and H. Kennedy, Proc. Natl. Acad. Sci. USA **110**, 5187 (2013).
[71] S. W. Oh, J. A. Harris, L. Ng, B. Winslow, N. Cain, S. Mihalas, Q. Wang, C. Lau, L. Kuan, A. M. Henry, M. T. Mortrud, B. Ouellette, T. N. Nguyen, S. A. Sorensen, C. R. Slaughterbeck, W. Wakeman, Y. Li, D. Feng, A. Ho, E. Nicholas, K. E. Hirokawa, P. Bohn, K. M. Joines, H. Peng, M. J. Hawrylycz, J. W. Phillips, J. G. Hohmann, P. Wohnoutka, C. R. Gerfen, C. Koch, A. Bernard, C. Dang, A. R. Jones, and H. Zeng, Nature **508**, 207 (2014).
[72] L. R. Varshney, B. L. Chen, E. Paniagua, D. H. Hall, and D. B. Chklovskii, PLoS Comput. Biol. **7**, e1001066 (2011).
[73] S. Achard and E. Bullmore, PLoS Comput. Biol. **3**, e17 (2007).
[74] H. Lange and S. Boese, in *Recurrence Quantification Analysis*, edited by C. L. Webber Jr. and N. Marwan, Understanding Complex Systems (Springer, Cham, CH, 2015), pp. 349–374.
[75] O. E. Rössler, Phys. Lett. A **57**, 397 (1976).
[76] J. F. Donges, J. Heitzig, R. V. Donner, and J. Kurths, Phys. Rev. E **85**, 046105 (2012).
[77] R. V. Donner, M. Small, J. F. Donges, N. Marwan, Y. Zou, R. Xiang, and J. Kurths, Int. J. Bifurcat. Chaos **21**, 1019 (2011).
[78] J. F. Donges, Y. Zou, N. Marwan, and J. Kurths, Europhys. Lett. **87**, 48007 (2009).
[79] M. Wiedermann, A. Radebach, J. F. Donges, J. Kurths, and R. V. Donner, Geophys. Res. Lett. **43**, 7176 (2016).
[80] E. Kalnay, M. Kanamitsu, R. Kistler, W. Collins, D. Deaven, L. Gandin, M. Iredell, S. Saha, G. White, J. Woollen *et al.*, B. Am. Meteorol. Soc. **77**, 437 (1996).
[81] J. Donges, R. Donner, K. Rehfeld, N. Marwan, M. Trauth, and J. Kurths, Nonlinear Proc. Geophys. **18**, 545 (2011).
[82] N. Marwan, J. F. Donges, Y. Zou, R. V. Donner, and J. Kurths, Phys. Lett. A **373**, 4246 (2009).
[83] M. Wiedermann, J. F. Donges, D. Handorf, J. Kurths, and R. V. Donner, Int. J. Climatol. **37**, 3821 (2017).
[84] J. Maluck and R. V. Donner, PLoS ONE **10**, e0133310 (2015).
[85] J. Runge, V. Petoukhov, J. F. Donges, J. Hlinka, N. Jajcay, M. Vejmelka, D. Hartman, N. Marwan, M. Paluš, and J. Kurths, Nat. Commun. **6**, 8502 (2015).
[86] M. Kretschmer, D. Coumou, J. F. Donges, and J. Runge, J. Climate **29**, 4069 (2016).
[87] D. Eroglu, N. Marwan, S. Prasad, and J. Kurths, Nonlin. Proc. Geophys. **21**, 1085 (2014).
[88] R. Jacob, K. Harikrishnan, R. Misra, and G. Ambika, Phys. Lett. A **380**, 2718 (2016).
[89] C. Zhou, L. Zemanová, G. Zamora-Lopez, C. C. Hilgetag, and J. Kurths, New J. Phys. **9**, 178 (2007).
[90] Z. Burda, J. Duda, J. M. Luck, and B. Waclaw, Phys. Rev. Lett. **102**, 160602 (2009).